

Chromatic patchy particles: effect of specific interactions on liquid structure.

Oleg A. Vasilyev,^{1,2} Boris A. Klumov,^{3,4,5} and Alexei V. Tkachenko⁶

¹*Max-Planck-Institut für Intelligente Systeme, Heisenbergstraße 3,
D-70569 Stuttgart, Germany*

²*IV. Institut für Theoretische Physik, Universität Stuttgart, Pfaffenwaldring 57,
D-70569 Stuttgart, Germany*

³*Joint Institute for High Temperatures, Moscow, Russia*

⁴*Institute for Information Transmission Problems, Moscow,
Russia*

⁵*Moscow Institute of Physics and Technology, Moscow,
Russia*

⁶*Center for Functional Nanomaterials, Brookhaven National Laboratory, Upton,
NY, USA*

(Dated: 6 December 2024)

We study the structural properties of patchy particle liquid, with special focus on the role of "color", i.e. specific interactions between individual patches. One experimental realization of such "chromatic" patchy particles is by decorating them with single-strained DNA linkers. The complementarity of the linkers will promote formation of bonds only between predetermined pairs of patches. By using the MD simulation, we compare local coordination, the short range order, and other structural properties of the aggregates formed by "colored" and "colorless" systems. The analysis is done for spherical particles with two different patch arrangement (tetrahedral and cubic). The additional color constraint results in a less connected liquid structure which is also less stable thermodynamically. From our data, we estimate the configurational entropy loss due coloring to be about $2k_B T$ per particle, which in turn should improve the relative stability of the corresponding ordered phases. Despite having slightly lower connectivity, the colored liquid exhibits significantly better local bond orientational order measured by PDFs of the Steinhardt's rotational invariants q_l and w_l . We associate this with lower strain due to the removed bonds.

PACS numbers: **82.70.Dd**, **07.05.Tp**, **61.43.Bn**

Keywords: patchy particles, self-assembling

I. INTRODUCTION

In the recent years, patchy particles have emerged as a key model system for advanced self-assembly¹⁻¹¹. These are typically micron-scale colloids featuring chemically distinct regions (patches) arranged in a pre-engineered pattern on the particle surfaces. In most cases, the patches preferentially attract each other resulting in strongly directional character of the interparticle interactions, reminiscent of the covalent bonding with predetermined bond orientations. Furthermore, by decorating patches with DNA molecules, one may introduce multiple types of them, and selective type-dependent binding³. This can be compared with coloring of the patches. One can expect that adding the "color" to directionality of interparticle interaction will result in a greater control of the resulting structure.

While the primary interest in patchy particles is due to their potential for programmable self-assembly of a great variety of ordered superlattices, the study of disordered phases in this class of systems is of great conceptual importance as well⁹⁻¹¹. In fact, such studies provide valuable insights both into the equilibrium phase behavior and kinetics of self assembly. For instance, Smallegange and Sciortino⁹ have recently demonstrated that the ground state of the system of patchy particles need not to be a crystal, even when the particles themselves are highly symmetric. Specifically, for the case of four-patch particles with tetrahedral symmetry, the diamond crystal is a thermodynamically preferred state only in the limit of a strong directionality of the bond, i.e. very small patch size. Otherwise, the system can achieve maximum connectivity without sacrificing all of its configurational entropy, i.e. preserving a liquid-like structure. A similar conclusion has been reached independently in our recent study¹¹ that preceded the current work. Rather than exploring the equilibrium phase behavior, we were interested in structural properties of patchy particle liquid. Remarkably, the four-patch system demonstrates relatively high degree of local ordering, as opposed to six-patch system with cubic symmetry. We explained this difference by the observation that disordered aggregates of a patchy system should typically have a coordination number close to $Z = 4$, subject to assumption that directionality of bonds is not extreme.

In the current work, we expand the previous analysis and study the effect of "chromatic" interactions between patches. It is expected that combining bond directionality with such selectivity (e.g., due to DNA functionalization of the patches) will result in higher order and programmability of the self-assembled structures. Similarly to our previous study, we analyse

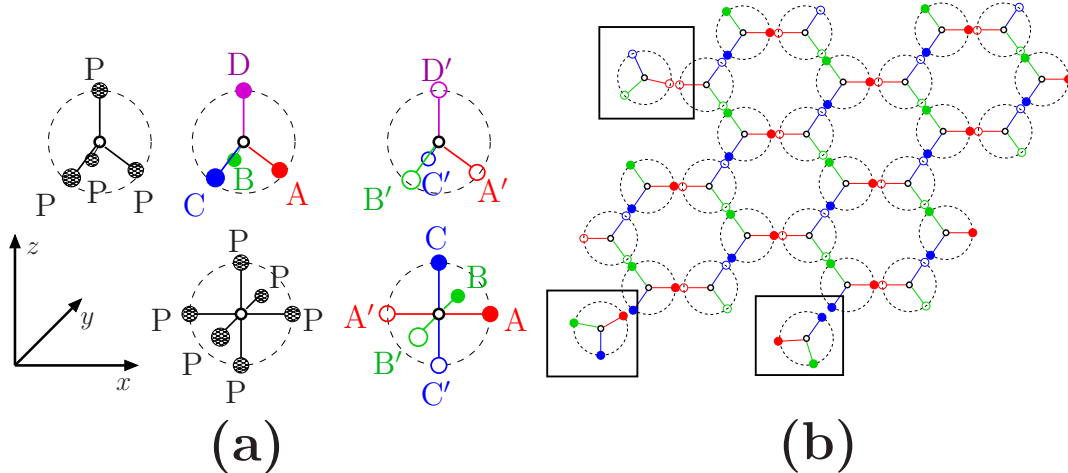


FIG. 1. (Color online) (a) Location of colorless (P) and colored primary (A, B, C, D) and complementary (A', B', C', D') patches for 4pch and 6pch particles; (b) Top view on layer of a perfect crystal for color 4pch system. Particles in black squares do not interact with the aggregate due to the rule of color interaction.

both 4 patch particles with tetrahedral symmetry (4pch) and 6 patch particles with cubic one (6pch). For each system we consider the extreme cases: all patches equivalent ("colorless"), and all patches on the same particle having different colors, subject to complementarity rule ("colored").

II. MODEL AND NUMERICAL ALGORITHM

In our numerical algorithm we consider a patchy particle as a solid sphere of radius R . Patches are attached to the surface of this sphere and rotate with it. Therefore, we should take into account rotational degrees of freedom. The motion of a single particle is represented as a combination of a translational displacement of the center of the particle and a rotation the particle around its center. We describe the rotational orientation of particles using quaternions.

We study the specific interactions between patches. In the colored case only the complementary patches AA' , BB' , CC' , and DD' attract each other. Interaction between other, non-complementary, pairs such as AA , AB' etc., are absent. In the colorless case, every pair of patches PP can interact.

At the initial time moment the orientation of k -th patch for j -th particle with respect

to its center is given by the vector $\mathbf{a}_j^{(k)}(0)$. The system of colored 4pch particles is binary. A "primary" 4pch particle has the patches at following positions: $\mathbf{a}_j^{(1)}(0) = \left(\sqrt{\frac{8}{9}}, 0, -\frac{1}{3}R\right)$ (A type), $\mathbf{a}_j^{(2)}(0) = \left(-\frac{\sqrt{2}}{3}R, \sqrt{\frac{2}{3}}R, -\frac{1}{3}R\right)$ (B type), $\mathbf{a}_j^{(3)}(0) = \left(-\frac{\sqrt{2}}{3}R, -\sqrt{\frac{2}{3}}R, -\frac{1}{3}R\right)$ (C type), and $\mathbf{a}_j^{(4)}(0) = (0, 0, R)$ (D type). A "complementary" particle is a mirror image of the "primary" ones, with patches A', B', C', D' located at positions A, C, B, D , respectively (see Fig. 1(a)). A colored 6pch particle has complementary patches located opposite to each other: $\mathbf{a}_j^{(1,2)}(0) = (\pm R, 0, 0)$ for A and A' , $\mathbf{a}_j^{(3,4)}(0) = (0, \pm R, 0)$ for B and B' , $\mathbf{a}_j^{(5,6)}(0) = (0, 0, \pm R)$ for C and C' , respectively.

The displacement of the center of the j -th particle at the time moment t is described by the vector $\mathbf{r}_j(t)$. Euler's rotation theorem tells us, that any displacement of a rigid body such that a point on the rigid body remains fixed, is equivalent to a single rotation at certain angle ϕ around some axis that runs through the fixed point. The orientation of j -th particle at the time moment t with respect to its center is given by the unit quaternion $\mathbf{\Lambda}_j(t)$. This quaternion has a form $\mathbf{\Lambda}_j(t) = [\cos(\phi_j/2), \sin(\phi_j/2)\mathbf{n}_j(t)]$, where the unit length vector $|\mathbf{n}_j(t)| = 1$ sets the axis passing through the center of the j -th particle and ϕ_j is the angle of rotation around this axis (see, e.g., Ref. 12). The conjugated quaternion is $\tilde{\mathbf{\Lambda}}_j(t) = [\cos(\phi_j/2), -\sin(\phi_j/2)\mathbf{n}_j(t)]$. The location of the k -th patch of the j -th particle at the time moment t is given by the formula $\mathbf{a}_j^{(k)}(t) = \mathbf{r}_j(t) + \mathbf{\Lambda}_j(t) \otimes \mathbf{a}_j^{(k)}(0) \otimes \tilde{\mathbf{\Lambda}}_j(t)$ where \otimes denotes the quaternion's product.

This approach may be used for molecular dynamic simulations of rigid objects¹³. In our model we have two types of the interaction. Patchy particles repel each other with soft-core central repulsion truncated potential

$$U(\mathbf{r}_{ij}) = \begin{cases} U_0(\mathbf{r}_{ij}) - U_0(r_c) + (r_c - |\mathbf{r}_{ij}|)U_0'(r_c), & \mathbf{r}_{ij} \leq 2R \\ 0, & \mathbf{r}_{ij} > 2R \end{cases}$$

where $U_0(\mathbf{r}_{ij}) = 4\epsilon_0 \left[\left(\frac{\sigma}{\mathbf{r}_{ij}}\right)^{12} - \left(\frac{\sigma}{\mathbf{r}_{ij}}\right)^6 \right]$ is the standard Lenard-Jones potential, $U_0'(r_c) = \left. \frac{dU_0(r)}{dr} \right|_{r=r_c}$ is its derivative, $\sigma = 2R$ is the interaction distance, $\epsilon_0 = 1$ is the interaction strength, $r_c = 2R$ is the cut-off distance, and $\mathbf{r}_{ij} = \mathbf{r}_i - \mathbf{r}_j$ is the vector, connecting centers of j -th and i -th particle. Patches of different particles attract each other with the Gaussian potential $U_G(\mathbf{a}_{ij}^{(kl)}) = -U_p e^{-\frac{(\mathbf{a}_{ij}^{(kl)})^2}{2w^2}}$, where $\mathbf{a}_{ij}^{(kl)} = \mathbf{a}_i^{(k)} - \mathbf{a}_j^{(l)}$ is a vector connecting a patch l of particle j and a patch k of particle i , $w = 0.2$ is the half-width of the interaction and U_p

is the strength of the interaction.

From the complete set of displacements and orientations of particles $\{\mathbf{r}_j, \mathbf{\Lambda}_j\}$ it is possible to compute a set of total forces and torques $\{\mathbf{F}_j, \mathbf{M}_j\}$ acting on every particles taking into account interactions between soft cores of particles and between pairs of complementary patches

$$\begin{cases} \dot{\mathbf{v}}_j(t) = \frac{1}{m}\mathbf{F}_j(\{\mathbf{r}_j, \mathbf{\Lambda}_j\}) \\ \dot{\omega}_j(t) = \frac{1}{I}\mathbf{M}_j(\{\mathbf{r}_j, \mathbf{\Lambda}_j\}) \end{cases}, \begin{cases} \dot{\mathbf{r}}_j(t) = \mathbf{v}_j(t) \\ \dot{\mathbf{\Lambda}}_j(t) = \frac{1}{2}\omega_j(t) \otimes \mathbf{\Lambda}_j(t) \end{cases}, \quad (1)$$

where I is the moment of inertia, $\dot{\mathbf{v}}_j$ and $\dot{\omega}_j$ are linear and angular accelerations, respectively. We use normalized units, the radius of particles is $R = 1$, the mass is $m = 1$, the moment of inertia of a solid sphere $I = \frac{2}{5}mR^2 = 0.4$.

The interaction with thermostat is realized in the form of Langevin equations $-\gamma\mathbf{v}_j(t) + \xi_j(t)$ and $-\frac{4}{3}\gamma R^2\omega_j(t) + \zeta_j(t)$ for forces and torques, respectively, where $\gamma = 6\pi\eta R$ is the friction coefficient for solvent viscosity η , $\xi_j(t)$ and $\zeta_j(t)$ are thermal noise terms with delta-correlated components $\langle \xi_i^\alpha(t)\xi_j^\beta(t') \rangle = 2\gamma k_B T \delta_{i,j} \delta_{\alpha,\beta} \delta_{t,t'}$, $\langle \zeta_i^\alpha(t)\zeta_j^\beta(t') \rangle = \frac{8}{3}\gamma R^2 k_B T \delta_{i,j} \delta_{\alpha,\beta} \delta_{t,t'}$. We use the constant temperature $k_B T = 1$ and friction $\gamma = 10$, therefore for times $t \gg 1/\gamma = 0.1$ the dynamics of a particle is Brownian. We simulate the system of $N = 1000$ particles in a cubic system of size $L = 48$ with periodic boundary conditions. The volume density for this system is $\rho = 4/3\pi R^3 N/L^3 \simeq 0.038$

The temperature is fixed to provide the constant diffusion coefficient. The state of the system is tuned by varying the strength U_p (measured in $k_B T$ units) of the attractive Gaussian potential (with the half-width $w = 0.2$) between appropriate patches. For small values of U_p the system is in the gas phase, for large values of U_p the system is in the gel-like state.

III. STRUCTURAL PROPERTIES

To define the local structural properties of the patchy system we use the bond order parameter method¹⁴, which has been widely used in the context of condensed matter physics¹⁴, hard sphere¹⁵⁻¹⁷ and Lennard-Jones systems¹⁸⁻²¹, complex plasmas²²⁻²⁵, colloidal suspensions^{26,27}, metallic glasses²⁸, confined films^{29,30}, granular media etc. Within this method the rotational invariants of rank l of both second $q_l(i)$ and third $w_l(i)$ order are calculated for each particle i in the system from the vectors (bonds) connecting its center

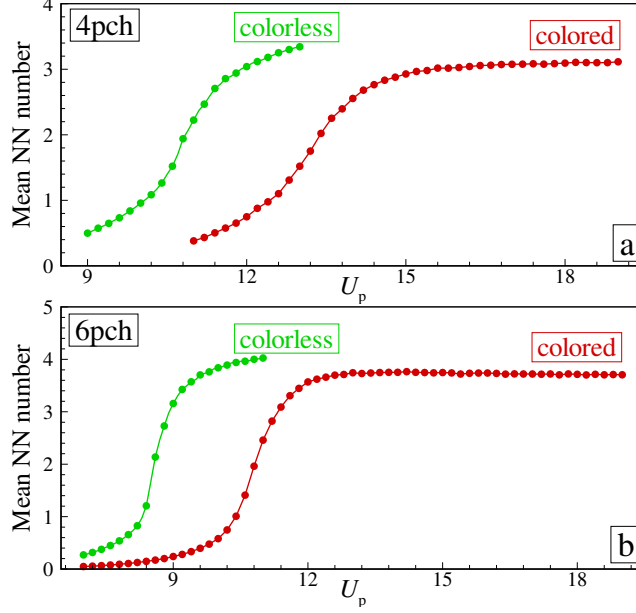


FIG. 2. (Color online) Mean value of topological nearest neighbors (NN) versus strength of the interaction U_p for colored (red curves) and colorless (green curves) systems. Presented are data for 4pch (a) and 6pch (b) systems.

with the centers of its $N_{\text{nn}}(i)$ nearest neighboring particles

$$q_l(i) = \left(\frac{4\pi}{(2l+1)} \sum_{m=-l}^{m=l} |q_{lm}(i)|^2 \right)^{1/2} \quad (2)$$

$$w_l(i) = \sum_{\substack{m_1, m_2, m_3 \\ m_1+m_2+m_3=0}} \begin{bmatrix} l & l & l \\ m_1 & m_2 & m_3 \end{bmatrix} q_{lm_1}(i) q_{lm_2}(i) q_{lm_3}(i), \quad (3)$$

where $q_{lm}(i) = N_{\text{nn}}(i)^{-1} \sum_{j=1}^{N_{\text{nn}}(i)} Y_{lm}(\mathbf{r}_{ij})$, Y_{lm} are the spherical harmonics and $\mathbf{r}_{ij} = \mathbf{r}_i - \mathbf{r}_j$ are vectors connecting centers of particles j and i . We note, that the bond order parameters $w_l \propto q_l^3$, so, in general, these parameters are much more sensitive to the local orientational order in comparison with q_l . Here, to define the structural properties of the patched particles, we calculate the rotational invariants q_l , w_l for each particle using the fixed number N_{nn} of the nearest neighbors (NN): $N_{\text{nn}} = 4, 6$ for the first shell of 4pch and 6pch systems; next nearest neighbors (NNN) of both systems has $N_{\text{nn}} = 12$. The first shells of the ideal 4pch and 6pch systems have cubic diamond (CD) and simple cubic (SC) lattices, respectively. The next nearest neighbors has face centered cubic (FCC) lattice for both types of ideal

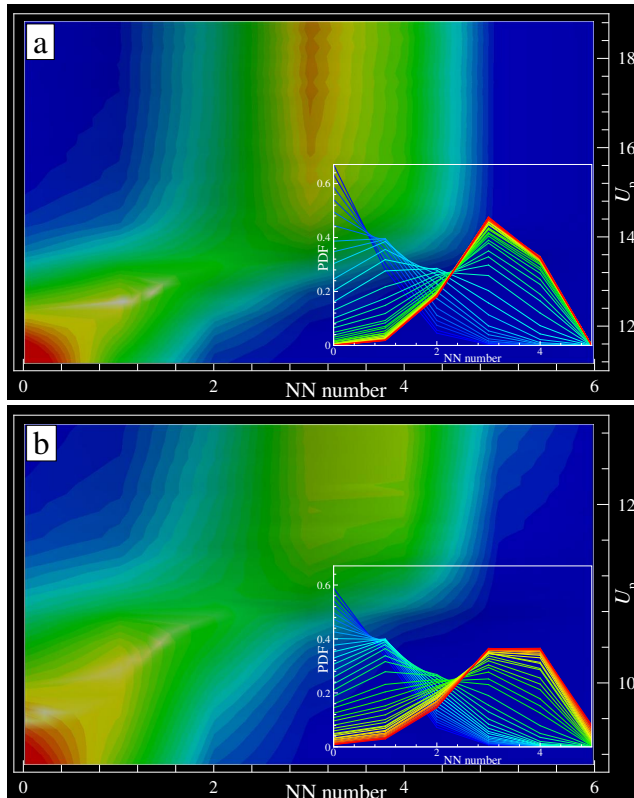


FIG. 3. (Color online) Patchy systems 4pch: the first shell analysis for the colored (a) and colorless (b) patchy systems. Probability distribution function (PDF) plotted versus number of the topological nearest neighbors (NN) and value of interaction strength U_p (the range of U_p is taken to cover gas, liquid-like and gel phases). Insets show the dependence of the PDFs on the NN for both colored (a) and colorless patchy (b) systems, respectively. The curves are color-coded via U_p value (red color corresponds to largest values of U_p).

patchy systems. We note, that formation of hexagonal diamond (HD) with hexagonal close packing (HCP) of the NNN is also possible for the patched system, at least kinetically.

The values of the different rotational invariants q_l and w_l for the perfect patchy crystals (for both NN and NNN) are shown in Table 1. A particle whose coordinates in the 4-dimensional space (q_4, q_6, w_4, w_6) are sufficiently close to those of the ideal lattice is counted as solid-like particle. By calculating the bond order parameters for the NNN it is easy to identify the disordered (liquid-like) phase as well.

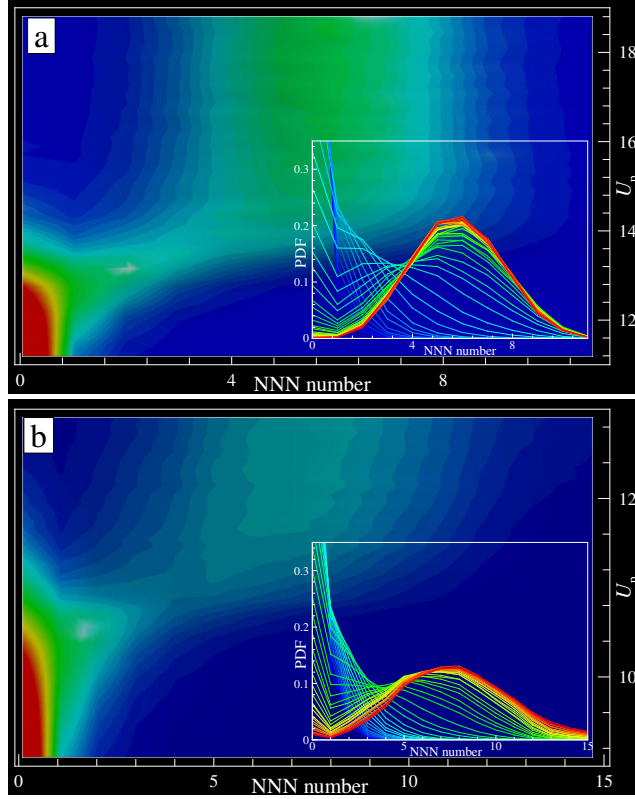


FIG. 4. (Color online) Patchy systems 4pch: the next nearest neighbors (NNN) analysis for the colored (a) and colorless (b) patchy systems. Probability distribution function (PDF) plotted versus number of next nearest neighbors (NNN) and value of interaction strength U_p (the range of U_p is taken to cover gas, liquid-like and gel phases). Insets show the dependence of the PDFs on the NNN for both colored (a) and colorless patchy (b) systems, respectively. The curves are color-coded via U_p value (red color corresponds to largest values of U_p).

TABLE I. Rotational invariants for the perfect patchy crystals

system structure	q_4	q_6	w_4	w_6
4pch CD, HD (1st shell, 4 NN)	0.509	0.628	-0.159	-0.013
6pch SC (1st shell, 6 NN)	0.76	0.35	0.159	0.013
4,6pch CD, SC (2nd shell, FCC)	0.191	0.575	-0.159	-0.013
4pch HD (2nd shell, HCP)	0.097	0.485	0.134	-0.012

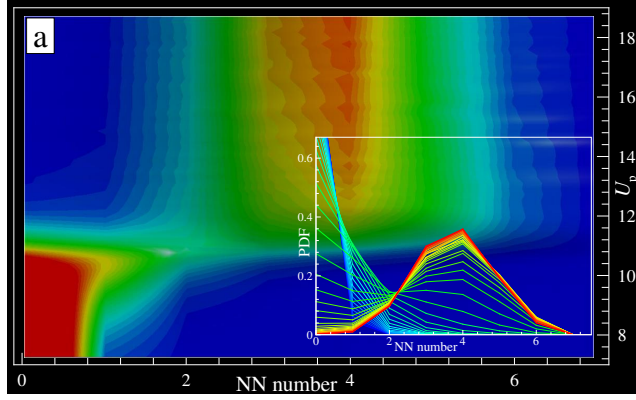


FIG. 5. (Color online) Patchy systems 6pch: the first shell analysis for colored (a) and colorless (b) patchy systems. Probability distribution function (PDF) plotted versus number of the topological nearest neighbors (NN) and value of interaction strength U_p (the range of U_p is taken to cover gas, liquid-like and gel phases). Insets show the dependence of the PDFs on the NN for both colored (a) and colorless patchy (b) systems, respectively. The curves are color-coded via U_p value (red color corresponds to largest values of U_p).

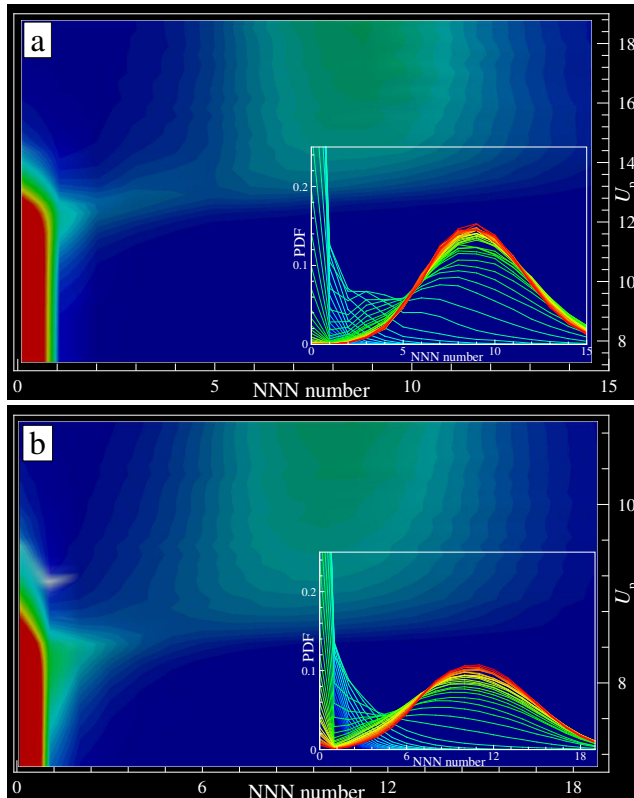


FIG. 6. (Color online) Patchy systems 6pch: the next nearest neighbors (NNN). analysis for colored (a) and colorless (b) patchy systems. Probability distribution function (PDF) plotted versus number of the topological next nearest neighbors (NNN) and value of interaction strength U_p (the range of U_p is taken to cover gas, liquid-like and gel phases). Insets show the dependence of the PDFs on the NNN for both colored (a) and colorless patchy (b) systems, respectively. The curves are color-coded via U_p value (red color corresponds to largest values of U_p).

IV. RESULTS OF SIMULATIONS

In Fig. 2 we plot the mean values of the number of topological nearest neighbors (NNs) as a function of the interaction potential U_p for 4pch (a) and 6pch (b) systems. The colored system exhibits aggregation at significantly higher interaction strength than the colorless one. This shift reveals an important information about the thermodynamics of the aggregated state that will be discussed in the final section. Note also that the average number of NNs, the mean coordination number saturates at a lower value for colored system than for colorless one.

Fig. 3 shows the influence of the color of the patches on the distribution of the number

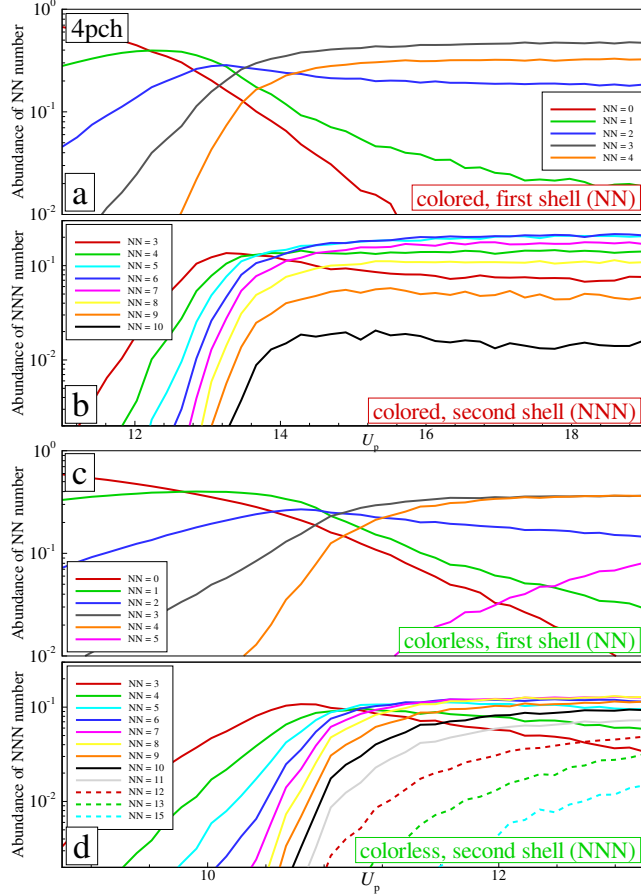


FIG. 7. (Color online) Patchy systems 4pch. Abundance of topological nearest neighbors (NN) number versus interaction strength U_p . The curves are color-coded via NN number (indicated on the plot). Data for the NN (a,c) and next nearest neighbors (NNN) (second shells) (b,d) are shown for both colored (a,b) and colorless (c,d) patchy systems. The quenching of particles having 3 and more patches, reflecting the sol-gel transition is clearly seen for both colored (observed at $U_p \simeq 13$) and colorless (observed at $U_p \simeq 11$) patchy systems.

of NNs for 4pch systems at different values of the interaction strength U_p . At low U_p both colored and colorless systems are in gas phase with number of NN close to zero. Increasing of U_p results in aggregation transition with the formation of a few amorphous clusters¹¹ with the nearly constant distribution of the topological NN. This transition is clearly seen in the Fig. 3 for both systems. Fig. 4 show the distributions of the number of the next nearest neighbors (NNNs) for the 4pch systems. Similar results for colored and colorless 6pch systems are presented in Fig. 5 and Fig. 6, for the first shell (NN) and the second shell (NNN) respectively.

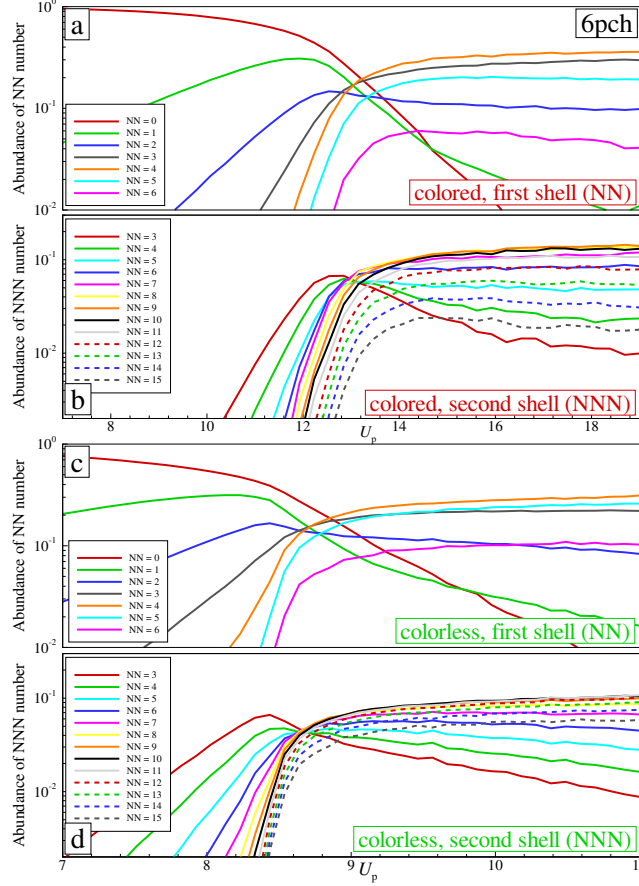


FIG. 8. (Color online) Patchy systems 6pch. Abundance of topological nearest neighbors (NN) number versus interaction strength U_p . The curves are color-coded via NN number (indicated on the plot). Data for the NN (first shell) (a,c) and next nearest neighbors (second shells) (b,d) are shown for both colored (a,b) and colorless (c,d) patchy systems. The quenching of particles with 4 and more patches, reflecting the sol-gel transition is clearly seen for both colored (observed at $U_p \simeq 13$) and colorless (observed at $U_p \simeq 8.5$) patchy systems.

An alternative representation of the above results is shown in Fig. 7 and Fig. 8, where the fraction of particles with different number of nearest and next nearest neighbors is plotted as a function of the interaction strength U_p for 4pch and 6pch systems, respectively.

Fig. 9 shows the radial distribution function $g(r)$ for 4pch and 6pch systems, for both colored (red curves) and colorless (green curves) at the gel phase state when the agglomeration of the particles is practically finished. Additionally, an important cumulative measure associated with $g(r)$ — mean number $N(< r)$ of particles inside a sphere of radius r : $N(< r) \equiv 4\pi\rho \int_0^r \xi^2 g(\xi) d\xi$ is shown on the plot by the same color as proper radial distri-

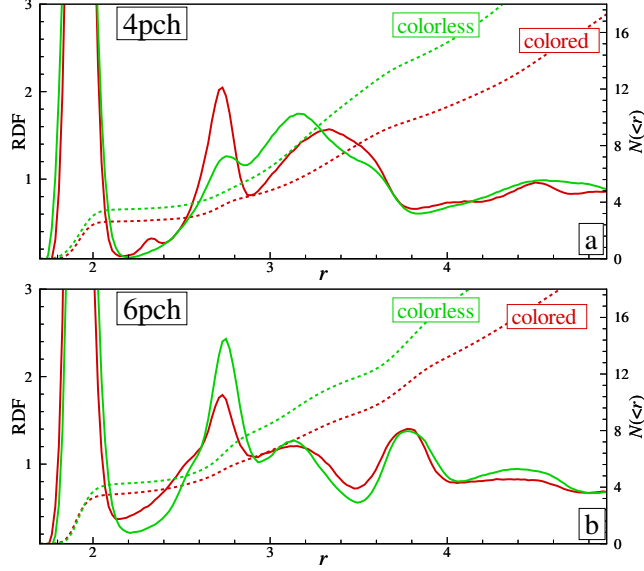


FIG. 9. (Color online) Radial distribution function $g(r)$ and its cumulative function $N(< r)$ ($N(< r) \equiv 4\pi\rho \int_0^r \xi^2 g(\xi) d\xi$), showing mean numbers of particles inside the sphere of radius r for colored (red curves) and colorless (green curves) systems with 4 (a) and 6 (b) patches at the gel phase state ($U_p \simeq 10 \div 15$). It is clearly seen that colorless patchy systems are a bit more dense than colored ones.

bution function $g(r)$. The analysis of the first coordination sphere reveals that the colorless patchy systems are somewhat more dense than colored ones, which is consistent with our observation that the colorless system is more connected

Structural properties of the particles, namely properties of the local orientational order are shown in Fig. 10 and Fig. 11 for 4pch and 6pch systems, respectively, for both colored (red curves) and colorless (green curves) systems at the final gel phase state. The probability distribution functions $P(q_l)$ and $P(w_l)$ of particles over different rotational invariants q_l and w_l ($l = 4, 6$) and its cumulative distributions being plotted reveal that colorless system is more ordered than colored one. Here, we calculated the PDFs $P(q_l)$ and $P(w_l)$ via using a fixed number of the nearest neighbors ($N_{\text{nn}} = 4$ and $N_{\text{nn}} = 6$ for the 4pch and 6pch system, respectively). Using of the topological NN change significantly the distributions; the effect is illustrated in Fig. 12, where the distribution $P(q_4)$ (calculated via number of the topological neighbors $N_{\text{nn}} = 3$) is plotted as a function of q_4 for both colored and colorless systems. Peaks observed on the red curve correspond to nearly perfect system with 3 patches. It is clearly seen, that in that case the colored system looks to be more ordered in comparison

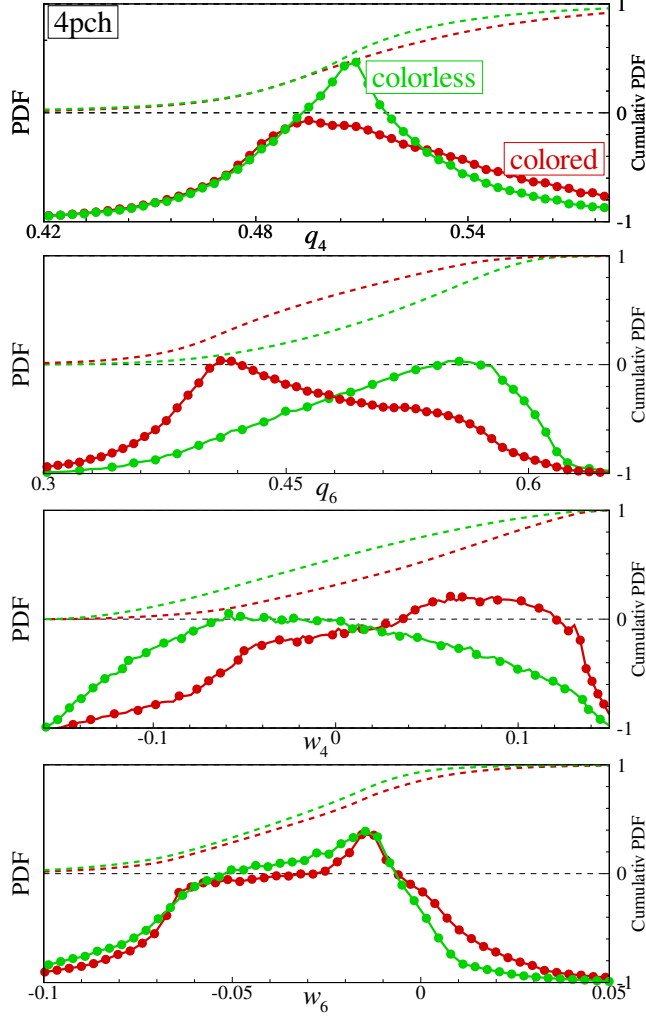


FIG. 10. (Color online) Patchy system 4pch. Probability distribution function $P(q_l)$ and $P(w_l)$ of particles over different rotational invariants q_l and w_l ($l = 4, 6$) calculated via fixed $N_{\text{nn}} = 4$ are plotted for both colored (red curves) and colorless (green curves) patchy systems. The curves reveal that colorless system is more ordered than colored one. Weak difference between the distributions $P(w_6)$ for both cases makes the bond order parameter w_6 to be a good measure to quantify the ordering.

with the colorless one.

V. DISCUSSION AND CONCLUSIONS

The detailed analysis of the liquid structure presented above gives a number of important insights into the physics of colored and colorless patchy system, and into difference between

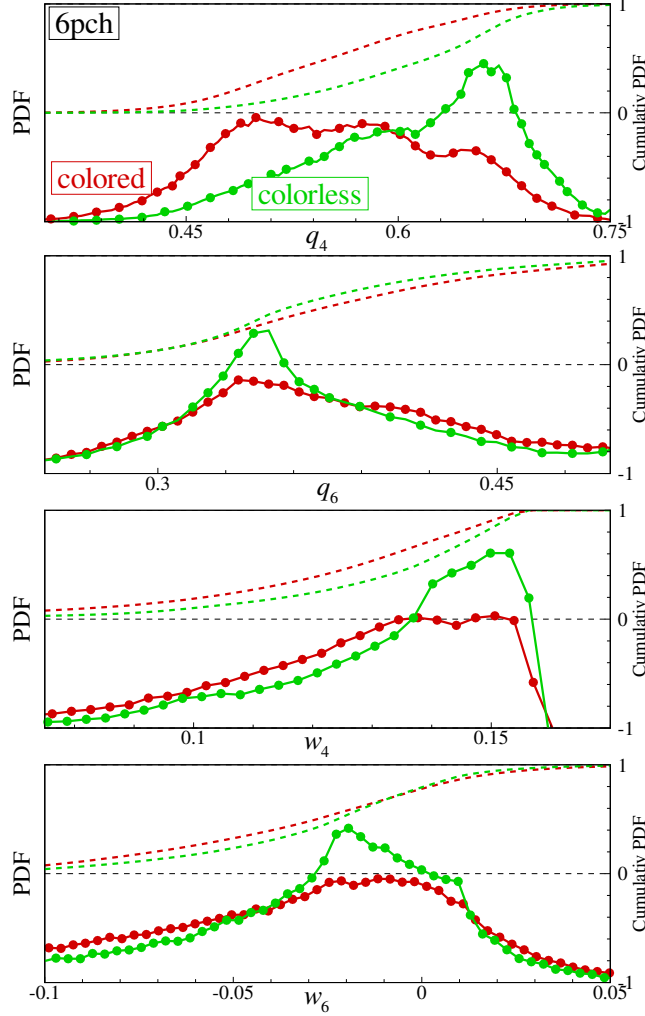


FIG. 11. (Color online) Patchy system 6pch. Probability distribution function $P(q_l)$ and $P(w_l)$ of particles over different rotational invariants q_l and w_l ($l = 4, 6$) calculated via fixed $N_{\text{nn}} = 6$ are plotted for both colored (red curves) and colorless (green curves) patchy systems. Like the system with 4 patches (see, Fig. 10), these curves also reveal more ordering of the colorless system in comparison with the colored one.

them.

In particular, the relative shift in Fig. 2 of the aggregation curves for colored and colorless systems can be attributed to a difference in their entropies. The aggregation occurs when the chemical potential in a condensed (liquid-like) phase is equal to that of a gas:

$$k_{\text{B}}T \log(C) = ST - \frac{k_{\text{B}}TZU_p}{2} \quad (4)$$

Here C is the particle concentration in the gas phase, S is entropy per particle in the

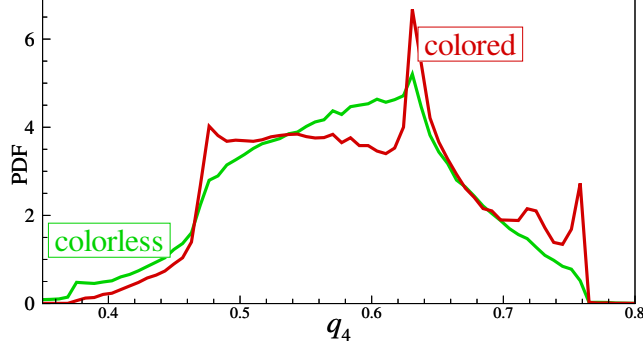


FIG. 12. (Color online) Patchy system 4pch. Probability distribution function $P(q_4)$ over bond order parameter q_4 (calculated via 3 topological nearest neighbors) for colored (red curve) and colorless (green curve) patchy systems at the gel state. Colored system looks to be more ordered than colorless one.

aggregate, and Z is the mean coordination number (number of NNs). By neglecting the difference in Z in aggregates of colored and colorless system, we conclude that the difference in entropy between them is proportional to shift of the aggregation point: $\Delta S = k_B Z \Delta U_p / 2$. This gives $\Delta S \simeq 4.5k_B$ for 4pch and $\Delta S \simeq 5k_B$ for 6pch. This difference can be partially attributed to trivial combinatorial effect: for each configuration of the colored system, there are 12 possible orientations of an individual colorless 4-patch particle and 24 such states in 6pch system. This accounts for $2.5k_B$ and $3.2k_B$ of the entropy difference, respectively. The rest of the difference, approximately $2k_B$ per particle should be attributed to the fact that there is a significantly smaller number of contact networks that respect complementarity rule of the colored system as compared to unconstrained networks of colorless patchy colloids. This is a very important observation from the point of view of thermodynamic stability of ordered self-assembled lattices. Indeed, this configuration entropy difference only affects the disordered liquid phase, but not the crystalline structure. As a result, the periodic lattice in the colored case is expected to gain a "bonus" free energy of approximately $2k_B T$ per particle, with respect to the liquid phase. This difference is due to suppressed entropy of the disordered state, subjected to color constraints.

Fig. 2 indicates only a minor difference in the maximum values of the mean coordination number Z between colored and colorless systems. However, the detailed analysis of PDFs of this parameter reveals a much greater contrast. For instance, the colored 4pch system is clearly dominated by particles with $Z = 3$, while its colorless counterpart has much larger

fraction of particles with completely saturated bonds, i.e. $Z = 4$. This must be a result of the greater constraints imposed by coloring of the patches. Interestingly, the better connected colorless system is not necessarily better ordered. Among several PDFs of rotational invariants that characterize the bond orientation order, we distinguish a striking example of $P(q_4)$ for subset of particles that have coordination number $Z = 3$. One can clearly see much better ordering in the colored system compared to colorless. The explanation of this is that the additional bonds that appear in colorless system came at the expense of additional deformation. Indeed, if we imposed a condition that each interparticle bond is perfectly aligned with the vector pointing towards the center of the patch, the maximum average coordination number that could be achieved were $Z = 5/3$. As we have discussed in the earlier work¹¹, this constraint is typically unrealistic, and the coordination number is expected to be larger (tending towards $Z = 4$, consistently with the present results). These additional bonds however do result in modest bond rotation and strain in the particle network. It is result of this deformation that leads to pronounced suppression of local order near $Z = 3$ particles in the better connected colorless system. On the other hand, the effects appears to be opposite for complete shells ($Z = 4$ and $Z = 6$ particles in 4pch and 6pch systems, respectively), as shown in Figs 10-11. While the local orientational order remains weak in all these cases, the peaks in PDFs are generally stronger for colorless systems.

The central conclusion of our study is that colored patches provide a important additional element of control over the self assembled structures. The fact that liquid structure is more constrained is expected to make ordered phases more stable compared to colorless case. In particular, we expect that limitation on patch size and the associated bond directionality found in Ref. 9 should be less severe for the colloids with colored patches.

This study is supported by European Research Council under FP7 IRSES Marie-Curie grants PIRSES-GA-2010-269139 and PIRSES-GA-2010-269181. Research carried out in part at the Center for Functional Nanomaterials, Brookhaven National Laboratory, which is supported by the U.S. Department of Energy, Office of Basic Energy Sciences, under Contract No. DE-AC02-98CH10886. BAK was supported by the Russian Science Foundation, Project no. 14-12-01185.

REFERENCES

- ¹S. C. Glotzer, & M. J. Solomon, *Nature Materials* 6 (2007) 557.
- ²V. N. Manoharan, M. T. Elsesser, & D. J. Pine, *Science* 301 (2003) 483.
- ³Y. Wang et al. *Nature* 491 (2012) 51.
- ⁴F. Romano, E. Sanz & F. Sciortino, *J. Chem. Phys.* 134 (2011) 174502.
- ⁵F. Romano, E. Sanz, and F. Sciortino, *J. Phys. Chem. B* 113 (2009) 15133.
- ⁶E. G. Noya, C. Vega, J. P. K. Doye, and A. A. Louis, *J. Chem. Phys.* 132 (2010) 234511.
- ⁷Z. Zhang, A. S. Keys, T. Chen, and S. C. Glotzer, *Langmuir* 21 (2005) 11547.
- ⁸N. Kern and D. Frenkel, *J. Chem. Phys.* 118 (2003) 9882.
- ⁹F. Smallenburg and F. Sciortino, *Nature Physics* 9 (2013) 554.
- ¹⁰D. de las Heras, J. M. Tavares, M. M. Telo da Gama Bicontinuous and mixed gels in binary mixtures of patchy colloidal particles *Soft Matter* 8, 1785-1794 (2012)
- ¹¹O.A. Vasilyev, B.A. Klumov, A.V. Tkachenko, *Phys. Rev. E* 88 (2013) 012302.
- ¹²D.J. Evans, *Mol. Phys.* 34 (1977) 317.
- ¹³D.J. Evans, S. Murad *Mol. Phys.* 34 (1977) 327.
- ¹⁴P. Steinhardt, D. Nelson, M. Ronchetti, *Phys. Rev. Lett.* 47 (1981) 1297; P. Steinhardt, D. Nelson, M. Ronchetti, *Phys. Rev. B* 28 (1983) 784.
- ¹⁵I. Volkov, et al., *Phys. Rev. E* 66 (2002) 061401.
- ¹⁶T. Aste, et al., *Physica A* 339 (2004) 16; T. Aste, *J. Phys.: Condens. Matter* 17 (2005) S2361.
- ¹⁷B. A. Klumov, S. A. Khrapak, and G. E. Morfill, *Phys. Rev. B* 83 (2011) 184105.
- ¹⁸P.R. ten Wolde, M. J. Ruiz-Montero and D. Frenkel, *J. Chem. Phys.* 104 (1996) 9932.
- ¹⁹M.D. Rintoul and S. Torquato, *J. Chem. Phys.* 105 (1996) 9528.
- ²⁰W. Lechner and C. Dellago, *J. Chem. Phys.* 129 (2008) 114707.
- ²¹B.A. Klumov, *JETP Lett.* 98 (2013) 259; B.A. Klumov, *JETP Lett.* 97 (2013) 372.
- ²²G.E. Morfill, et al., *Contrib Plasma Phys.* 44 (2004) 450.
- ²³B. Klumov et al., *Plasma Phys. and Controll. Fusion* 51 (2009) 124028.
- ²⁴B. Klumov et al., *EPL* 92 (2010) 15003.
- ²⁵B.A. Klumov, *Phys. Usp.* 53 (2010) 1053.
- ²⁶U. Gasser, E. R. Weeks, A. Schofield et al, *Science* 292 (2001) 5515.
- ²⁷T. Kawasaki and H. Tanaka, *J. Phys.: Condens. Matter* 22 (2010) 232102.

²⁸A. Hirata et al., Science 341 (2013) 376.

²⁹B.A. Klumov and G.E. Morfill, JETP Lett. 85 (2007) 498; B.A. Klumov, G.E. Morfill, JETP 107 (2008) 908.

³⁰Y. Peng et al., Phys. Rev. E 83 (2011) 011404.